ACOUSTIC RADIATION FROM HONEYCOMB SANDWICH PLATES

K. H. Heron
Aerodynamics Department,
Royal Aircraft Establishment,
Farnborough, Hampshire, England

FIFTH EUROPEAN ROTORCRAFT AND POWERED LIFT AIRCRAFT FORUM
SEPTEMBER 4 – 7TH 1979 - AMSTERDAM, THE NETHERLANDS

ACOUSTIC RADIATION FROM HONEYCOMB SANDWICH PLATES

K. H. Heron
Aerodynamics Department,
Royal Aircraft Establishment,
Farnborough, Hampshire, England

ABSTRACT

The growing use of honeycomb sandwich panels in helicopter cabins is liable to increase the level of internal noise. High stiffness-to-weight ratios imply structures with a low acoustic transmission loss and a high acoustic radiation efficiency. Without reducing the static bending stiffness, honeycomb sandwich panels can be designed, with low core shear stiffnesses. Such panels do not exhibit the bad acoustic properties described above.

This paper shows how the acoustic properties can be predicted for a given panel. A set of experiments is described, using five different honeycomb sandwich panels, and the results are shown to agree well with prediction.

The most important conclusion is that as the core shear stiffness is changed from high values through to low, the acoustic properties go from medium to bad to good. If possible low core shear panels should be used, but if this is not possible, then high core shear panels should be used. Panels in between, as defined in the body of this paper, must be avoided.

ACOUSTIC RADIATION FROM HONEYCOMB SANDWICH PLATES

K. H. Heron
Aerodynamics Department,
Royal Aircraft Establishment,
Farnborough, Hampshire, England

1 INTRODUCTION

The growing use of honeycomb sandwich panels in aircraft design presents the acoustician with increasing problems. High stiffness-to-weight ratios imply structures with a low transmission loss (TL) and a high acoustic radiation efficiency. Kurtze and Watters[1] in 1959 suggested that a sandwich panel could be designed to have high stiffness statically, or at low frequencies, whilst becoming more compliant at the higher acoustic frequencies. A number of authors have considered the problem since 1959[2-6], but unfortunately most of them have concentrated on thick compressible cores such as foam. This has led to the dilational modes, or double-wall resonances, having national frequencies sufficiently low to influence the results considerably. With honeycomb cores which are designed to have a high compressible stiffness, such dilational modes have high natural frequencies and can be ignored.

This paper shows how the original concept of Kurtze and Watters can be applied to modern honeycomb sandwich panels.

Section 2 deals with the basic theory and explains how the important acoustic properties of sandwich panels can be predicted. Section 3 describes the experimental apparatus and shows how the various results can be interpreted. Section 4 compares these results with the theory of section 2 and, finally, section 5 discusses the implications of the theory.

2 THEORY

From Kurtze and Watters[1] the following equation can be derived for the flexural wave speed in a honeycomb sandwich panel,

$$X^3 + \alpha\beta_0 X^2 - \beta_0 X - \alpha\beta_0\beta_\infty = 0 \qquad (1)$$

where

$$\beta_0 = B_0\omega^2/\mu c^4 \quad , \qquad (2)$$

$$\beta_\infty = B_\infty\omega^2/\mu c^4 \quad , \qquad (3)$$

$$\alpha = \mu c^2/Gd \quad , \qquad (4)$$

and

$$X = c_p^2/c^2 \quad . \qquad (5)$$

μ is the total panel mass per unit area, G is the core shear modulus, d is the core depth, c_p is the panel flexural wave speed, c is the speed of sound in air and ω is the radian frequency. Also

$$B_0 = E'\left((d + 2h)^3 - d^3\right)/12 \quad , \qquad (6)$$

$$B_\infty = E'h^3/6 \qquad (7)$$

and

$$E' = E/(1 - \nu^2) \quad . \qquad (8)$$

h is the thickness of each skin, and E and ν are respectively the Young's modulus and Poisson's ratio for the skin material.

In deriving equation (1) the following assumptions have been made:-

(a) all three layers are constructed of isotropic materials;
(b) the core does not contribute directly to the flexural stiffness of the composite plate;
(c) all three layers move in phase, that is there are no dilational modes;
(d) B_∞ is negligible in comparison to B_0 .

It is worth noting at this stage that for large α or large ω , $X^2 \approx \beta_\infty$, which can be shown to imply that the core is only acting as extra weight. For small α or small ω , equation (1) reduces to $X^2 \approx \beta_0$, which shows that the core is still doing its usual job of acting as a spacer and forcing the skins into tension and compression.

The *radiation ratio*, σ , is defined as the acoustic power radiated by the plate into half space, divided by the acoustic power that a piston of the same area would radiate if it were vibrating with the same rms velocity. It was first evaluated by Maidanik[7] for simply supported thin isotropic plates. With Crocker's[8] corrections and some modifications it can be recast as follows.

$$\sigma = \begin{cases} \dfrac{64c^2}{A\pi^2\omega^2} g_1(X) + \dfrac{Pc}{\pi A\omega} g_2(X) & \text{for } X < 1 \quad (9) \\ \max\left(\dfrac{Pf_c}{c}, \sqrt{10}\right) & \text{for } X = 1 \quad (10) \\ \left(X/(X-1)\right)^{\frac{1}{2}} & \text{for } X > 1 \quad (11) \end{cases}$$

where

$$g_1(X) = \begin{cases} \dfrac{X^{3/2}(1-2X)}{(1-X)^{\frac{1}{2}}} & \text{for } X < \tfrac{1}{2} \quad (12) \\ 0 & \text{for } X > \tfrac{1}{2} \quad (13) \end{cases}$$

and

$$g_2(X) = \frac{X\left[(1-X)\ln\left((1+\sqrt{X})/(1-\sqrt{X})\right) + 2\sqrt{X}\right]}{(1-X)^{3/2}} . \quad (14)$$

A and P are the plate area and perimeter respectively, X is obtained from solving equation (1), and f_c can be obtained by solving equation (1) for ω when $X = 1$. The modifications to the standard formula at $X = 1$ are suggested by the author so as to blend better with the formulae for $X \neq 1$. For $X < 1$ the standard formula has been doubled to account for clamped rather than simply supported edges.

The *power ratio*, γ , is defined as the acoustic power radiated by the plate divided by the total power dissipated by the plate under point mechanical excitation.

$$\gamma = \frac{2\eta_{PR}}{\eta_P + 2\eta_{PR}} , \quad (15)$$

where

$$\eta_{PR} = \frac{\rho c}{\mu\omega}\sigma , \quad (16)$$

and $$\eta_P = 2\xi \quad . \tag{17}$$

η_{PR} is the coupling loss factor between the plate and a reverberant room, η_P is the energy loss factor and ξ is the plate damping ratio.

The transmission loss, TL , can be predicted from the formula

$$\tau = \frac{4\rho^2 c^2}{\omega^2 \mu^2}\left[\sqrt{10} + \frac{2\pi^2 c^2}{A\omega}\,\frac{n_P \sigma^2}{\eta_{PT}}\right] \tag{18}$$

where $$\eta_{PT} = \eta_P + 2\eta_{PR} \quad ,$$

$n_P(\omega)$ is the radian modal density of the plate and

$$TL = -10 \log_{10}(\tau) \quad . \tag{19}$$

The $\sqrt{10}$ of equation (18) comes from the assumption of field incidence for the mass law. The plate modal density n_P can be calculated as follows. If K_P is the plate wave number then

$$n_P(\omega) = \frac{A}{2\pi} K_P \frac{\partial K_P}{\partial \omega} \tag{20}$$

and hence

$$n_P(\omega) = \frac{A\omega}{4\pi^2 c^2 X}\left[2 - \frac{\omega}{X}\frac{\partial X}{\partial \omega}\right] \tag{21}$$

with X given by equation (1).

This would conclude the theoretical section if the plate could be assumed symmetric in the two in-plane directions. However, honeycomb core does not have a symmetrical construction, to the extent that the core shear modulus, G , in different directions varies by a factor of about 2. The direction of highest G will be designated longitudinal and the perpendicular direction of lowest G will be designated lateral. In order to take account of this asymmetry it is proposed that for the three variables σ, γ and τ , the average of the maximum and the minimum predicted values are used. It should be noted that this does not mean simply averaging the results obtained assuming longitudinal and lateral G values; results corresponding to intermediate values of G can and do produce maxima for a given frequency.

3 EXPERIMENTAL DETAILS

The experiments were conducted using a reverberant room of volume $V = 64\ m^3$. The various test plates were held in a 70kg frame which was inset on anti-vibration mounts into a wall of the room. The plates were hard bolted every 8 cm to the frame to achieve a nearly fully fixed edge constraint. The plates were rectangular of size 1.4 m × 0.9 m. Nine 0.5g accelerometers were attached at random positions to each plate in turn and five microphones were positioned randomly about the room.

The following tests were conducted. Firstly, a mechanical exciter was attached to a corner of the plate; secondly, this exciter was repositioned to shake a corner of the frame and thirdly, a loudspeaker was used in the room.

In all these tests, one-third-octave white noise was used as the generating signal, with centre frequencies between 250 Hz and 6300 Hz. The energy

levels deduced from the nine accelerometer readings were averaged to give a spatially averaged result. The five microphone readings were similarly treated. In all cases, the source was subsequently switched off allowing a check to be made on the background noise levels. Furthermore, for the mechanical excitation tests, the exciter was also run at the same electrical current level but mechanically disconnected, enabling the exciter self noise to be checked. If a difference of less than 10 dB was obtained between the check result and the test result, then the latter was discarded. The room reverberation time, T_R , was also measured with each plate in position.

The results from either mechanical excitation test can be used to deduce a measurement of σ , using

$$\sigma = \frac{13.8V\omega^2}{T_R A\rho^2 c^3} \frac{S_P}{S_a} \tag{22}$$

where S_p and S_a are the measured, spatially averaged, mean square, pressure and acceleration results.

It is also possible to show that the power ratio is given by

$$\gamma = \frac{\mu A\rho}{\pi^2 c n_p} \frac{S'_a}{S'_P} \tag{23}$$

where S'_a and S'_p are the acceleration and pressure results obtained using the acoustic excitation. Finally the total damping of the plate, ξ_T , can also be deduced, since

$$\xi_T = \tfrac{1}{2}\eta_{PT} = \frac{\rho c}{\mu\omega} \frac{\sigma}{\gamma} \quad . \tag{24}$$

It should be noted that it is usually necessary to correct the accelerometer results for the effect of the accelerometer mass, m , using the formula

$$K = 20 \log_{10}\left[1 + \frac{\omega m}{Z}\right] \quad , \tag{25}$$

where K is the dB correction and Z is the plate impedance. However with the plates described herein and 0.5g accelerometers the maximum value of K is about 1 dB and hence no corrections for this effect have been made.

4 RESULTS

Before discussing the more complicated results from sandwich plates, it is instructive to consider the results from a simple 2.5 mm thick aluminium plate. These are shown in Fig 1. The upper graph shows good agreement between theory and experiment for the radiation ratio, σ . The middle graph for the power ratio, γ , also shows good agreement, but it should be noted that theory must assume a value for ξ , the damping ratio. The value of 0.1% was chosen, which matches up fairly well with the total damping results shown in the lower graph. It is also interesting to note that the acoustic damping results, which can be deduced directly from σ , are close enough to the total damping results, to suggest the possibility that for this plate, acoustic damping is an important contributor to the total plate damping. This would imply a power ratio approaching unity, which is also evident from the middle graph.

Five sandwich plates, constructed from resin impregnated paper honeycomb cores with aluminium skins, were tested. The parameters of the plates, which are

labelled A, B, C, D and E are given in Table 1. The most important parameter is the shear ratio, α, which influences the flexural wave speed as given by equation (1). Plates A and B can be regarded as having low shear ratios, with plates D and E having high shear ratios. Fig 2 shows the radiation ratio results for all five plates. The agreement between theory and experiment is good, the rather arbitrary averaging process necessary to account for the asymmetry of the core in the theory appears to be satisfactory.

Considering Fig 1, the results for plates A, B and C may appear a little surprising. However, assuming longitudinal values, plates A and B have coincidence frequencies around 1000 Hz, whereas assuming lateral values, their coincidence frequencies are around 10000 Hz. Hence for frequencies in between there exists a possible value of G, the core shear modulus, for which coincidence occurs, and this phenomenon accounts for the high values of the radiation ratio. On the other hand, for plates D and E, all possible values of G lead to high coincidence frequencies.

Fig 3 shows the measured damping ratio for the five plates. The total damping results are shown as a range, because equations (23) and (24) involve n_p, the plate modal density, and n_p is a function of G. Plate A, and to some extent plates B and C, show acoustic damping playing a significant role, whereas plates D and E are controlled by mechanical damping. Overall a mechanical damping value of 1% seems to fit the results.

Assuming this mechanical damping ratio of 1%, Fig 4 shows the results for the power ratio. Here an average modal density was used to allow a single point result for each frequency. The agreement between theory and experiment is again good. Considering that the modal densities used to produce Fig 4 vary by as much as 10 from low to high frequencies, and that reciprocity has had to be assumed throughout, the agreement is very encouraging.

5 DISCUSSION

The theory presented in section 2 has been checked against experimental results and gave good agreement with both σ and γ. Since equation (18) for τ only assumes in addition that the free-field incidence mass law applies, it is evident that for the type of plates tested, the theory for σ, γ and τ with $\xi = 1\%$ is accurate enough for qualitative if not precise quantitative prediction.

Honeycomb sandwich plates can, effectively, be put into three acoustic categories.

$$\text{I} \qquad \alpha_{max} < 0.8 \tag{26}$$

$$\text{II} \qquad \alpha_{min} < 1 \,, \quad \alpha_{max} > 1 \tag{27}$$

$$\text{III} \qquad \alpha_{min} > 1.2 \tag{28}$$

where α_{min} and α_{max} can be taken as equal to the values of α in the longitudinal and lateral directions. For example plates R, S and T of Table 1 are in categories I, II and III respectively.

Fig 5 shows the predicted values of radiation ratio, power ratio and transmission loss for plates R, S and T. Since both plates R and S have high values of σ, they are dominated by acoustic rather than mechanical damping, and hence they exhibit high power ratio values. On the other hand, plate T shows a relatively low power ratio. The transmission loss results require some explanation, since at first sight it seems strange that plates R and S should be so different when their values of both σ and γ are similar. The reason lies

with their modal densities; in predicting σ and γ modal density is not involved, whereas in TL predictions the modal density is important. For plate R the modal density does not change much over the frequency range of interest, whereas the modal density of plate S increases by a factor of 10. The difference in transmission loss between plates R and T is mainly a reflection of their different radiation ratios.

The two parameters that ultimately matter from an acousticians point of view are γ and TL . Hence category II plates should be avoided, and where possible category III plates used in preference to category I.

Finally it should be noted that because aluminium honeycomb cores have high values of core shear stiffness, there appears to be no possibility of designing for category III plates made from such cores. Indeed, even for resin impregnated honeycomb cores, it is only just possible to design practical plates in category III; one such is plate T of Table 1.

6 CONCLUSIONS

Honeycomb sandwich plates, using resin impregnated paper cores and aluminium skins, can be designed with a sufficiently low core shear stiffness, so as to exhibit acceptable acoustic properties from the standpoint of the noise control engineer.

This paper shows how the acoustic properties can be predicted for a given plate. A set of experiments is also described, and the results are shown to agree well with prediction.

The most important conclusion is that as the core shear stiffness is changed from high values through to low, the acoustic properties go from medium to bad to good. If possible low core shear plates should be used, but if this is not possible, then high core shear plates should be used. Plates in between, as defined in the body of this paper, must be avoided.

REFERENCES

1) G. Kurtze and B.G. Watters, New wall design for high transmission loss or high damping, JASA 31, 739-748 (1959)

2) R.D. Ford, P. Lord and A.W. Walker, Sound transmission through sandwich constructions, J. Sound Vib 5, 9-21 (1967)

3) C.P. Smolenski and E.M. Krokosky, Dilational-mode sound transmission in sandwich panels. JASA 54, 1449-1457 (1973)

4) C.L. Dym and M.A. Lang, Transmission of sound through sandwich panels, JASA 56, 1523-1532 (1974)

5) M.A. Lang and C.L. Dym, Optimal acoustic design of sandwich panels, JASA 57, 1481-1487 (1975)

6) C.L. Dym, C.S. Ventres and M.A. Lang, Transmission of sound through sandwich panels: a reconsideration, JASA 59, 364-367 (1976)

7) G. Maidanik, Response of ribbed panels to reverberant acoustic fields, JASA 34, 809-826 (1962)

8) M.J. Crocker and A.J. Price, Sound transmission using statistical energy analysis, J. Sound Vib 9, 469-486 (1969)

Table 1

	PLATE	A	B	C	D	E	R	S	T	UNITS
a	length	1.4	1.4	1.4	1.4	1.4	1.4	1.4	1.4	m
b	width	0.9	0.9	0.9	0.9	0.9	0.9	0.9	0.9	m
d	core thickness	13	13	13	13	13	10	10	10	mm
	core density	48	48	48	48	48	24	24	24	kg/m^3
G	core shear modulus long	53	53	53	53	53	250	60	25	MN/m^2
	core shear modulus lat	28	28	28	28	28	130	31	13	MN/m^2
h	each skin thickness	0.4	0.6	0.9	1.6	2.5	0.5	0.5	0.5	mm
B_0	flexural stiffness	2.9	4.4	7.0	13.7	24.2	2.2	2.2	2.2	KN m
μ	mass/unit area	3.34	4.54	6.29	10.34	15.62	3.0	3.0	3.0	Kg/m^2
α	shear ratio long	0.56	0.76	1.06	1.73	2.62	0.14	0.58	1.39	
	shear ratio lat	1.06	1.44	2.00	3.28	4.96	0.27	1.12	2.67	

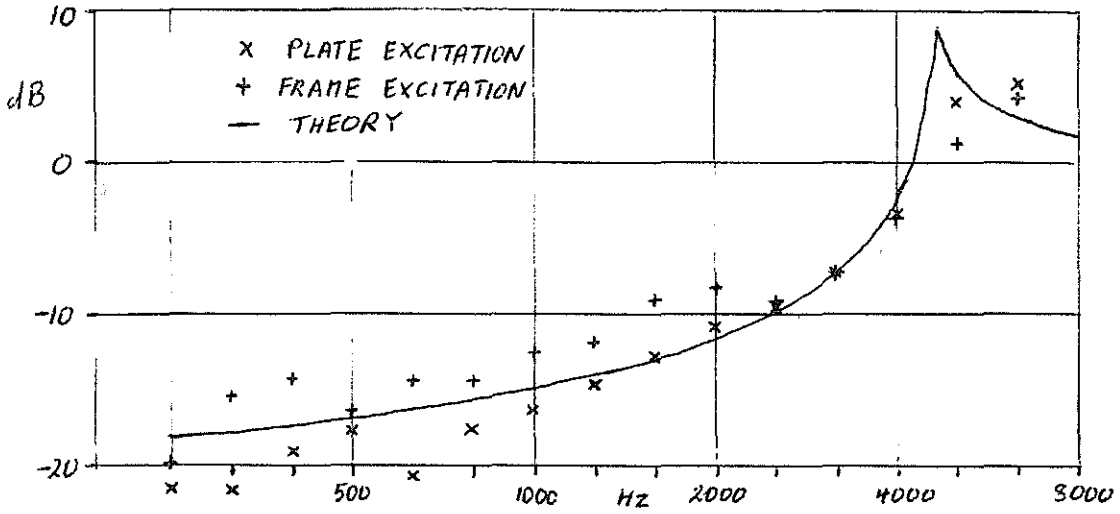

radiation ratio

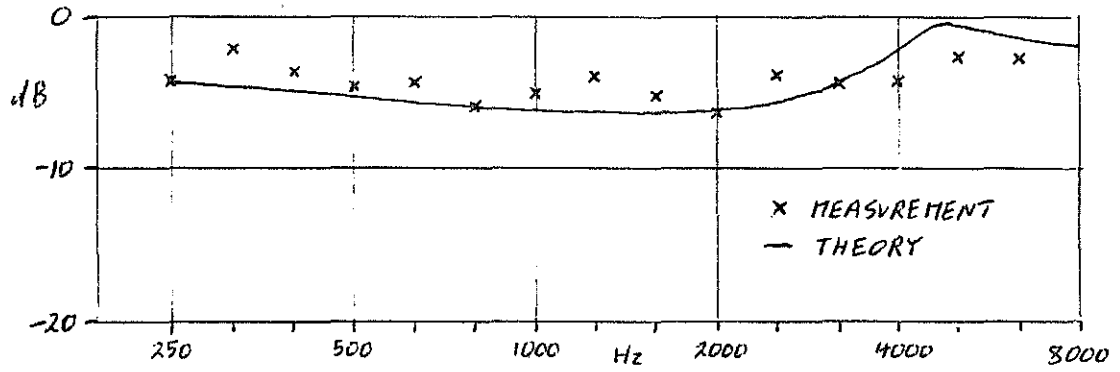

power ratio

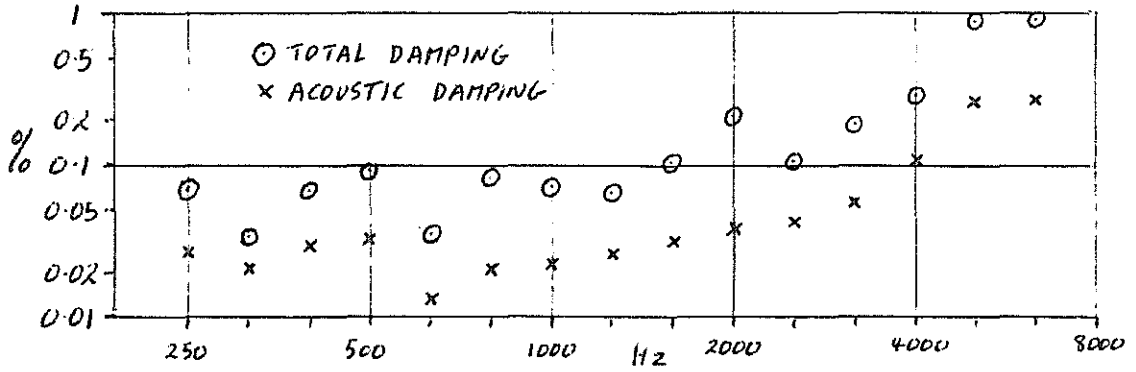

plate damping ratio

Fig 1 2.5mm aluminium plate

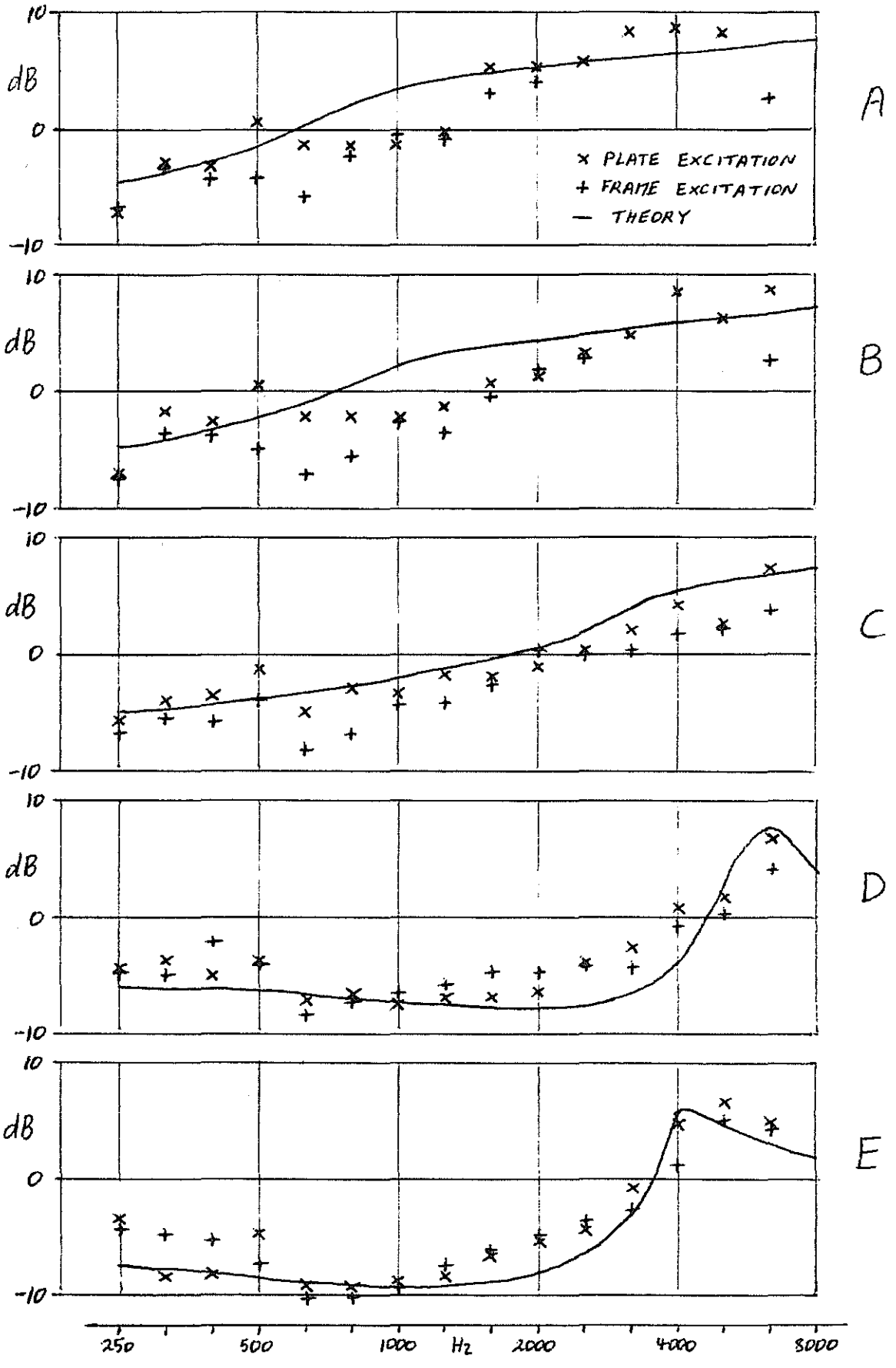

Fig 2 Radiation ratio

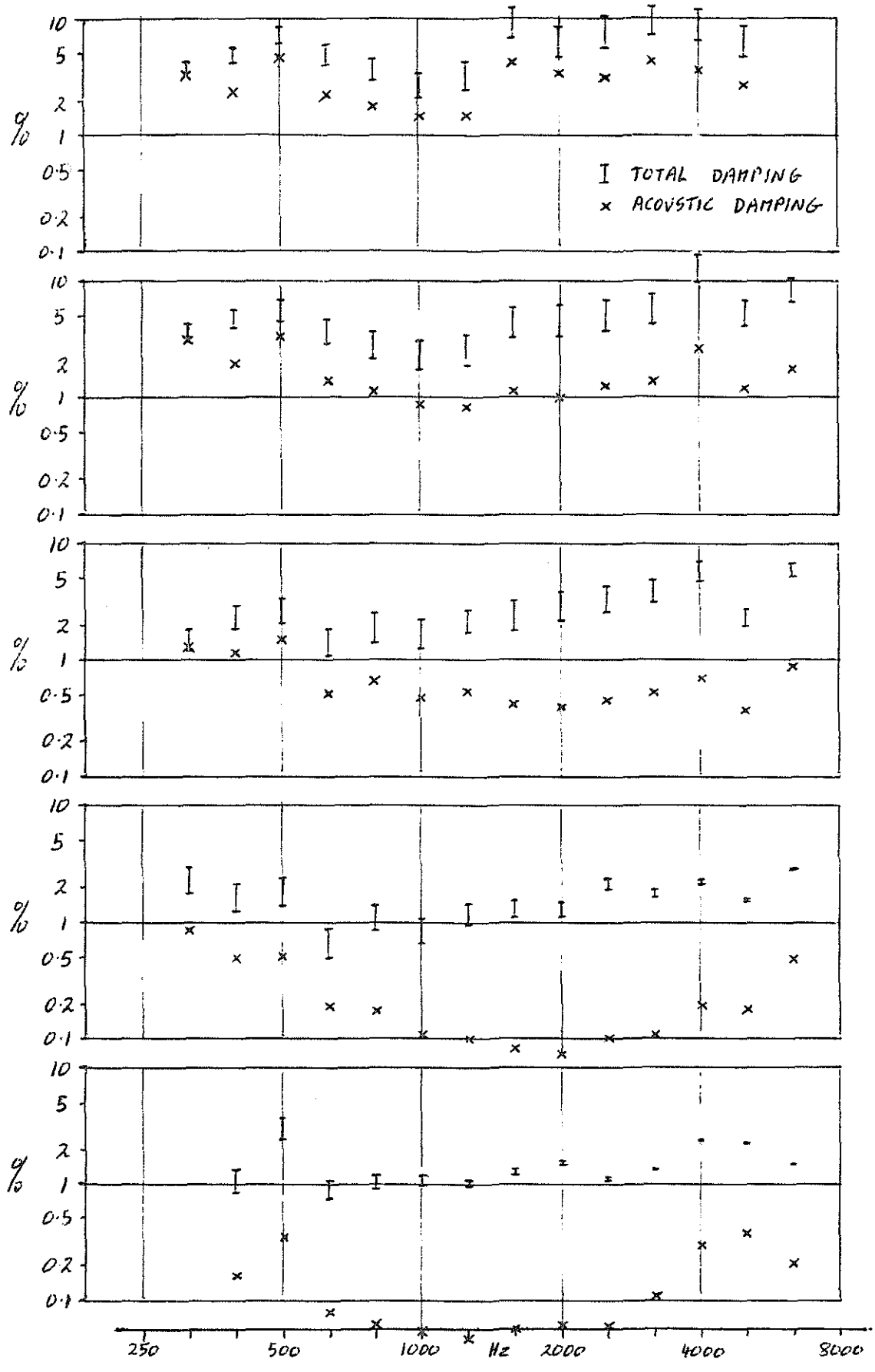

Fig 3 Plate damping ratio

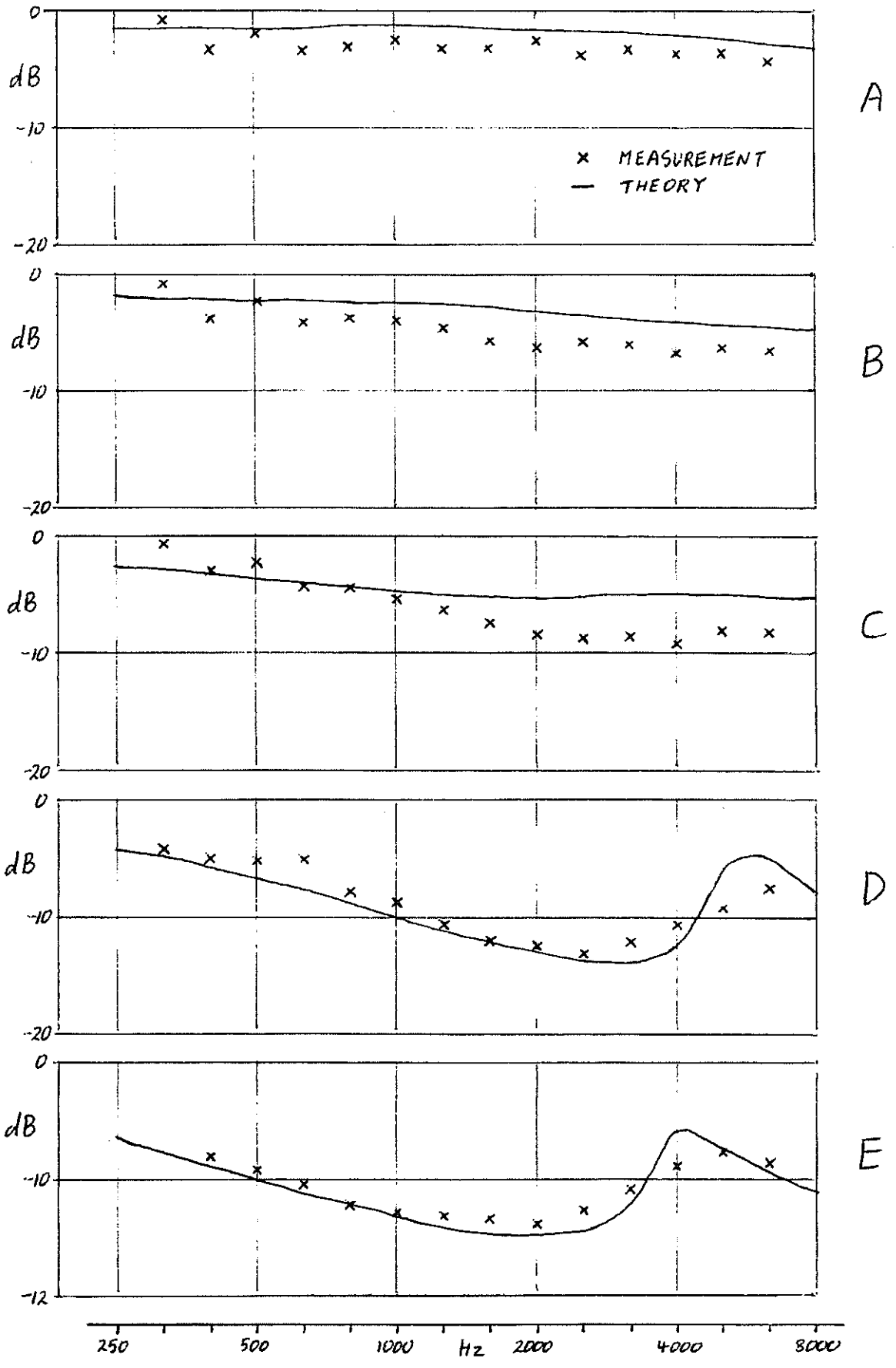

Fig 4 Power ratio

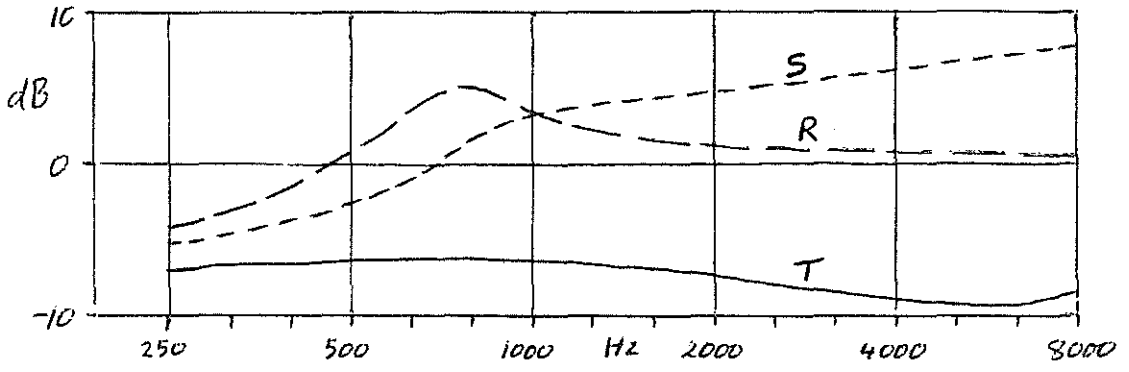

radiation ratio (σ)

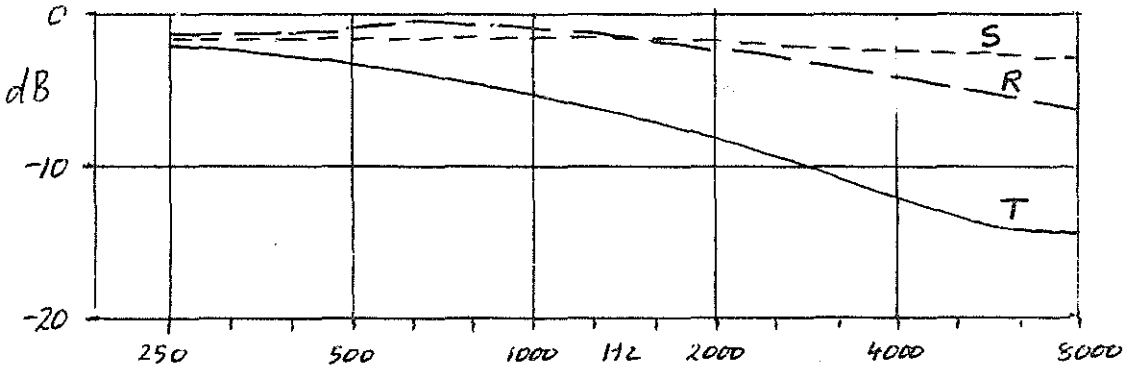

power ratio (γ)

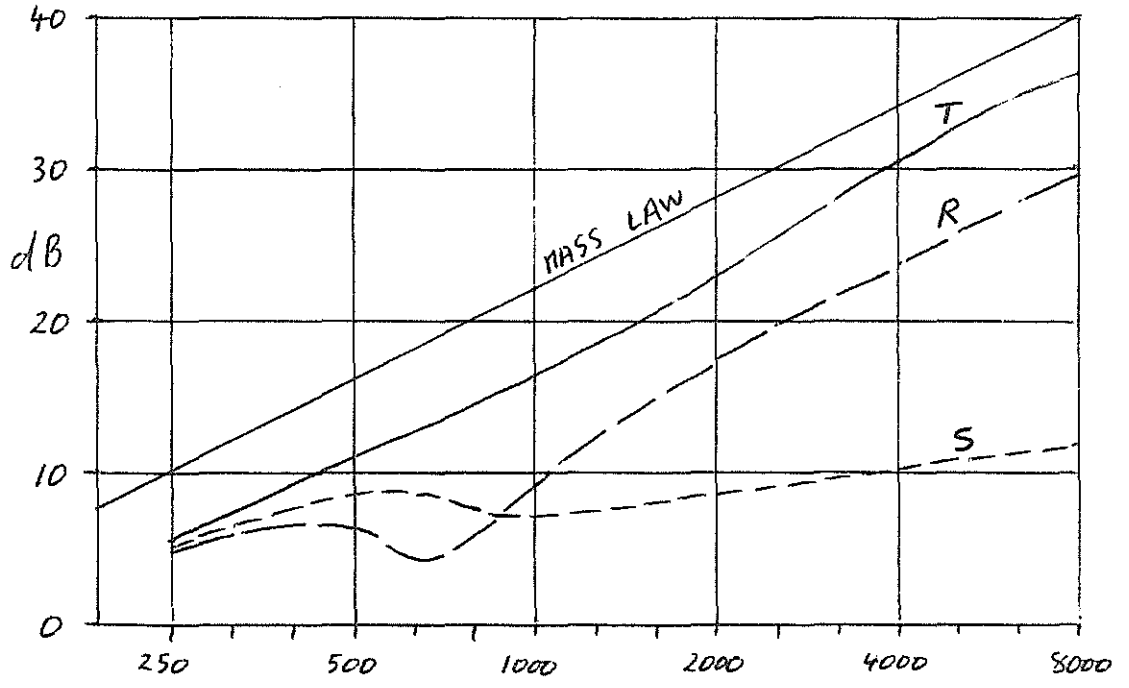

transmission loss (TL)

Fig 5 Plates R, S and T